Supplemental Information

Capturing membrane phase separation by dual resolution molecular dynamics simulations

Yang Liu, [1] A.H. de Vries,[1] Weria Pezeshkian[1], and Siewert J. Marrink[1,*]

[1]Groningen Biomolecular Sciences and Biotechnology Institute and the Zernike Institute for Advanced Material, University of Groningen, Groningen, The Netherlands

*Correspondence: s.j.marrink@rug.nl

Containing supporting Figures S1-S10, supporting Tables S1-S2, and supporting Methods (Recalibration of the hybrid model).

Supporting Methods: Recalibration of the VS hybrid scheme

We have applied the VS hybrid scheme on the ternary mixture (DPPC, DLiPC and cholesterol) at 295K to investigate the phase separation. However, although the cholesterol flip-flop is limited (see Methods), coupling the two different resolutions still resulted in a unusual interdigitation between the two leaflets, shown in Figure S1a. The cholesterol from the AA leaflet is found embedded deeply into the CG leaflet. It appears that the attraction between the AA cholesterol and CG leaflet is too strong. The underlying reason can be found in the different CG bead densities of the two cholesterol models. In Figure S2, the bond distance distributions of the CG virtual sites of cholesterol in the AA leaflets are computed and compared with their counterparts of the CG leaflets using the indicated mapping. Note, the bonds far from the resolution interface are not taken into consideration. As expected, apart from the C1 and C2 bonds, the rest of bond distributions in CG cholesterol (especially the ring structure) disagree with VS of AA cholesterol. The modified VS (CG) bond distances of the AA model causes the wrong local density of interaction sites and entails the risk of compromising the trends of free enthalpy and partitioning behavior against the standard CG model[1]. This could explain the strong interdigitation between CG and AA leaflets in the ternary membrane.

To solve the unusual interdigitation, we applied a scaling factor of 0.6 on the epsilon of the LJ potential between the subset of the VS beads in AA cholesterol (R3-R5 beads) and the C4 beads of DLiPC lipids in the CG leaflet. As shown in Figure S1b, the interdigitation is now much more realistic, although there are still one or two cholesterols translocated along the perpendicular direction of the membrane toward the CG leaflet. This result indicates that the strong attraction between AA cholesterol and the CG leaflet is the reason for excessive interdigitation in VS hybrid ternary membrane, and also that the scaling factor of 0.6 is not enough. Besides, this approach only reduces the attractions between cholesterol and DLiPC, while the attractions between cholesterol and DPPC are kept unchanged. This setup artificially increases the cholesterol partitioning into the ordered phase.

As it can be seen from Figure S2, some of the CG bonds are longer than the AA (VS) bonds, while for the others, the trend goes opposite. Thus, there is no uniform scaling factor of the attractions between the cholesterol and the other leaflet. To avoid rebuilding either the AA or CG cholesterol model, we next tried an approach in which the C6 of the LJ potential between the cholesterols (R3-R5 beads) and the other leaflet is set to 0, while keeping the C12 unchanged. Thus,

the flip-flop and vertical translocation of cholesterol is further suppressed while the interactions neither in AA nor in CG resolution are affected. To check the effects of this modification on the bilayer properties, we tested the VS hybrid scheme on pure DLiPC, DPPC/CHOL and DLiPC/CHOL membranes at 295K and compared the membrane properties against their corresponding references. As shown in Table S1, the area per lipid, and membrane thickness in AA, CG and VS hybrid models agree well for DLiPC and DPPC/CHOL membranes. In the case of the DLiPC/CHOL membrane, the properties of the VS hybrid membrane agree with the AA simulation, however, the difference between AA and CG resolutions is bigger. A similar picture emerges from comparison of the density profiles and the deuterium order parameter (Figure S3). Since the properties of the hybrid membrane agree better with the AA simulation (Table S1), further analysis will focus on the AA components in VS GROMOS/Martini hybrid model. In addition, we compare the DLiPC and DLiPC/CHOL membrane properties with other fully AA simulations in Table S2. We found that the area per lipid of DLiPC/CHOL membranes simulated using an in-house GROMOS force field (applied in our hybrid scheme and described in [2]) agrees well with the membrane simulated using other force fields. However, the area per lipid of DLiPC obtained by simulation using different forcefields is significantly different.

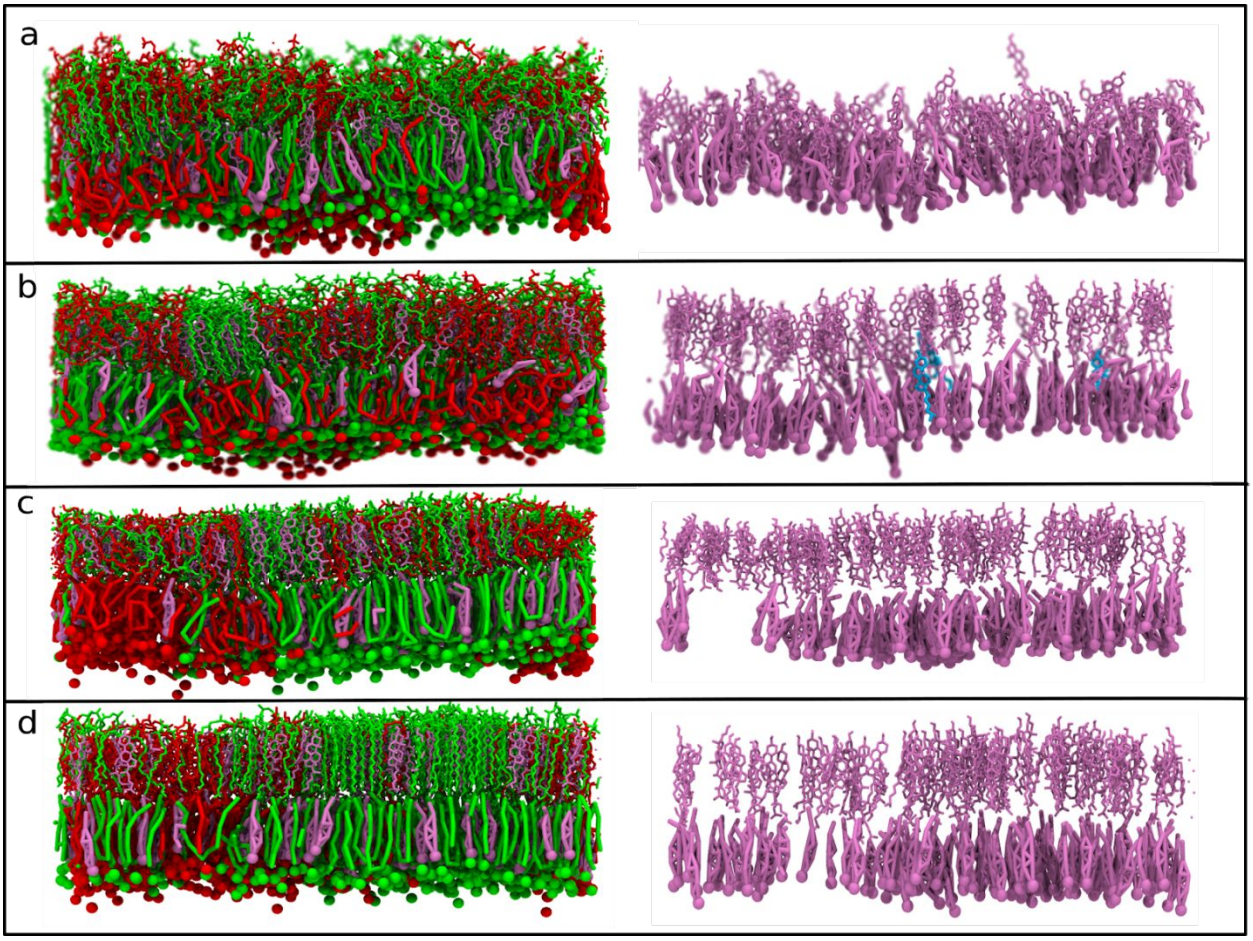

Figure S1. Snapshots of ternary membranes. (a) and (b) represent the original VS hybrid system and the scaled VS hybrid system, respectively. In the scaled hybrid system, the attractions between cholesterol (R3-R5 beads) in AA leaflet and the DLiPC lipids in the other CG leaflet are scaled down by a factor of 0.6. (c) and (d) represent the VS hybrid systems starting from half phase-separated phase and already phase-separated phase after about 10 μs, respectively. The C6 of the LJ potential between the cholesterols (R3-R5 beads) and the other leaflet is set to 0. The right column only shows the cholesterols of the ternary membranes in the left column and cholesterol in the wrong position is rendered in cyan in (b). DPPC, DLiPC and cholesterol are represented by green, red, and magenta, respectively. Thin and thick lines represent the AA and CG resolutions, respectively. Water is not shown for clarity.

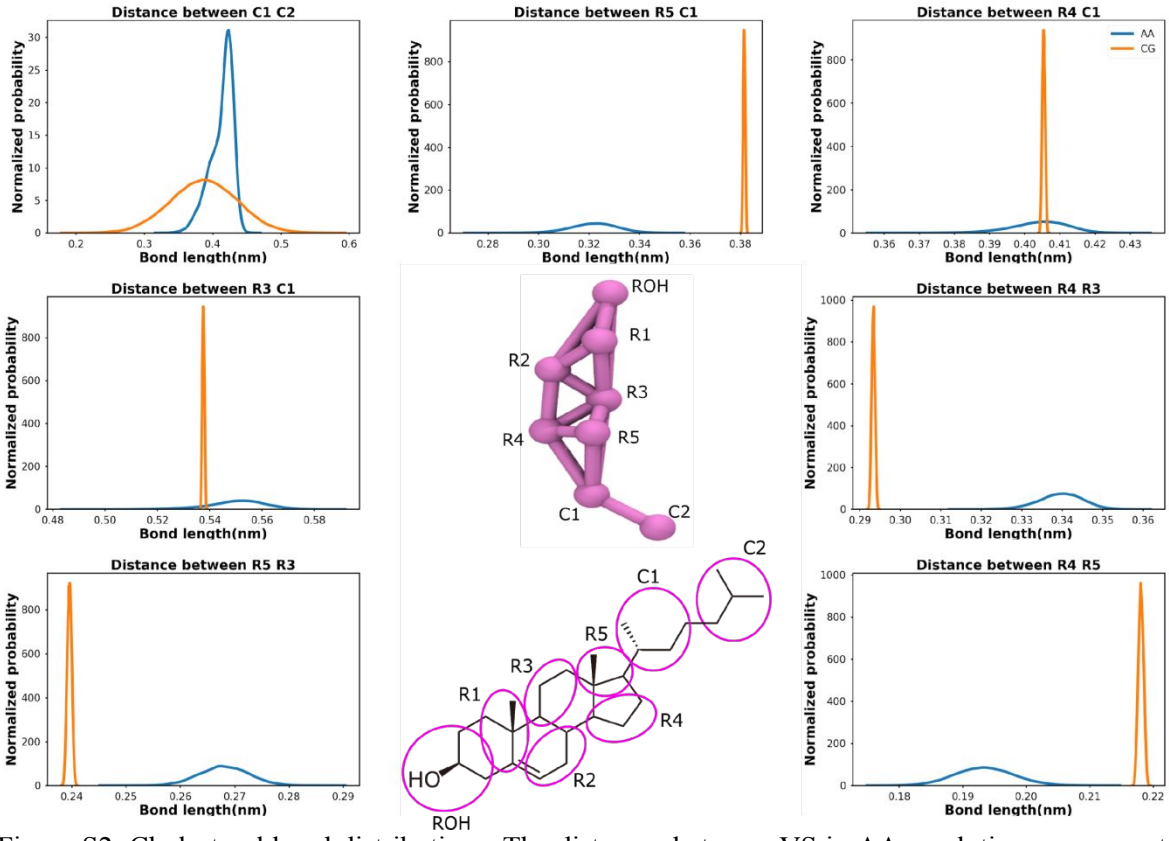

Figure S2. Cholesterol bond distributions. The distances between VS in AA resolution are computed and compared with the CG counterparts. Only the bonds close to the resolution interface are taken into consideration. A CG cholesterol structure and corresponding mapping scheme are shown in the middle.

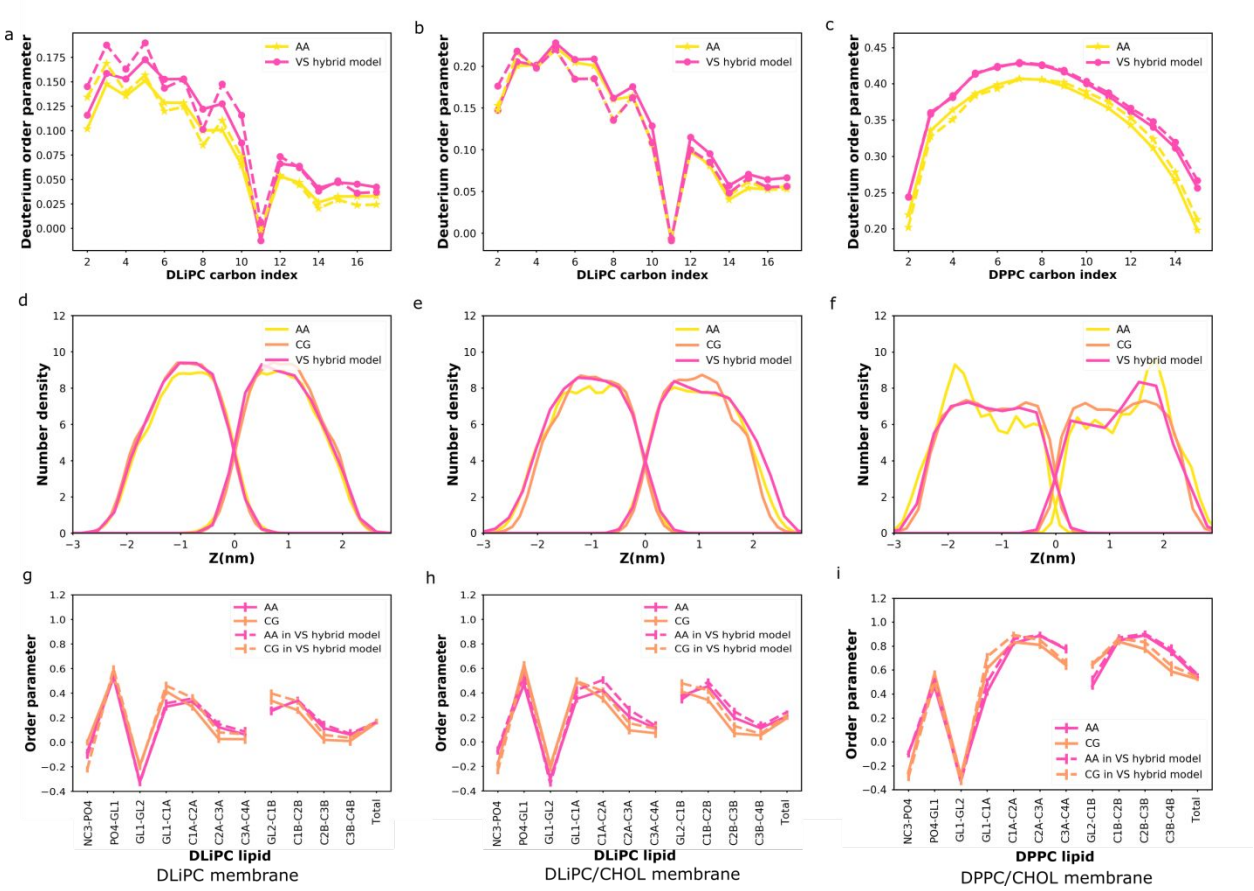

Figure S3. Membrane properties in different resolutions. (a-c) show the deuterium order parameter of pure AA simulation and AA components in the VS hybrid simulation. Solid and dashed lines represent two tails of the PC lipids, respectively. (d-f) represent the partial number density of VS and CG beads in membranes. The scaled Martini potential was applied in the VS hybrid model. (g-i) illustrate the CG (VS) order parameter in pure CG and AA simulation, as well as CG and AA components in the VS hybrid simulation. Panel (g-h) and (i) represent the order parameter of DLiPC and DPPC lipids in CG level, respectively. In AA models or AA components in hybrid models, the VS beads are used to compute the order parameter.

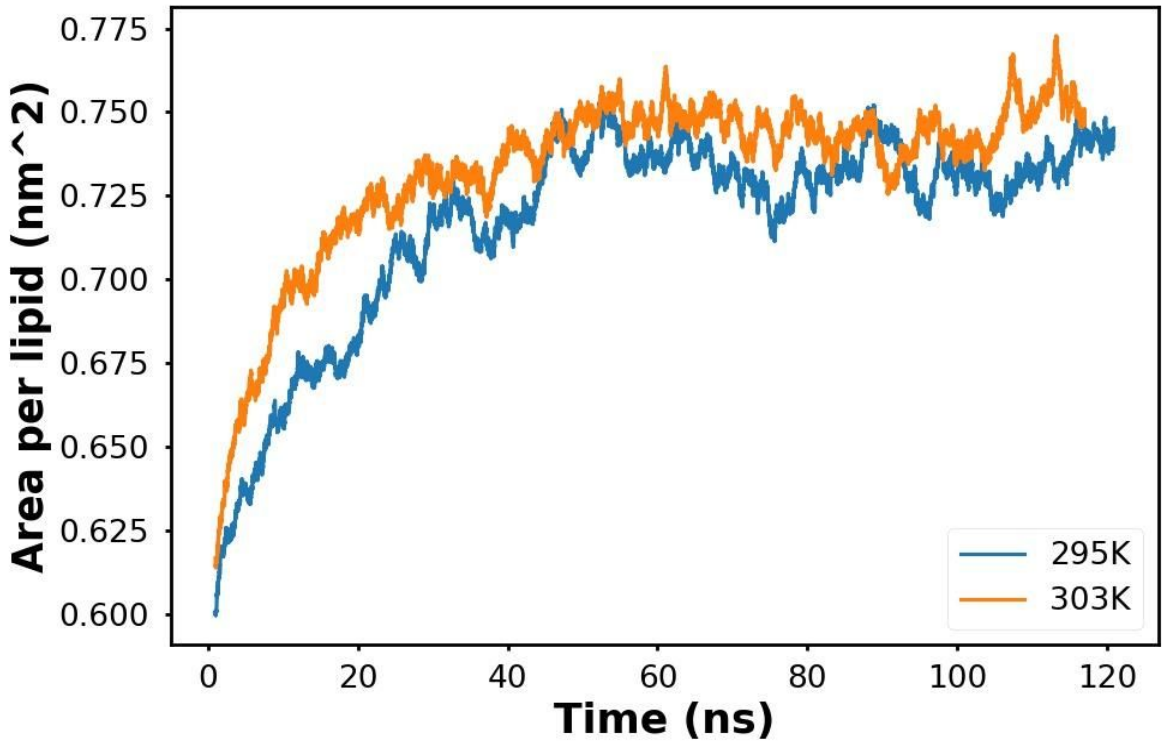

Figure S4. Area per lipid as a function of time. The systems are composed of 200 DLiPC lipids and simulated with the in-house GROMOS force field.

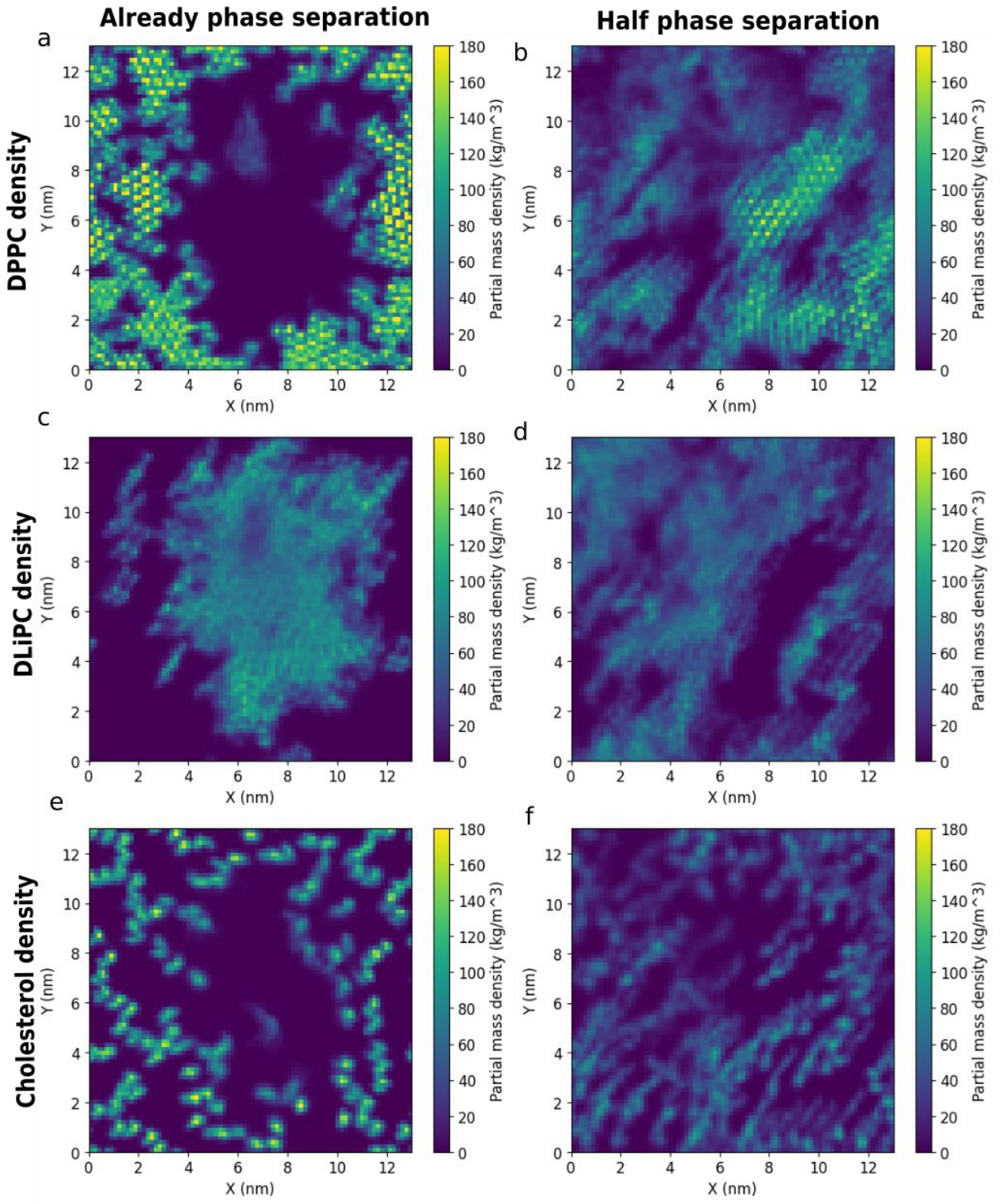

Figure S5. Density landscape of ternary membranes. The density landscape only considered the AA leaflets in the VS hybrid models. The tail and linker parts of PC lipids and whole cholesterols are regarded as references to compute the density maps. Landscapes are sampled from 9.5 μs to 10 μs.

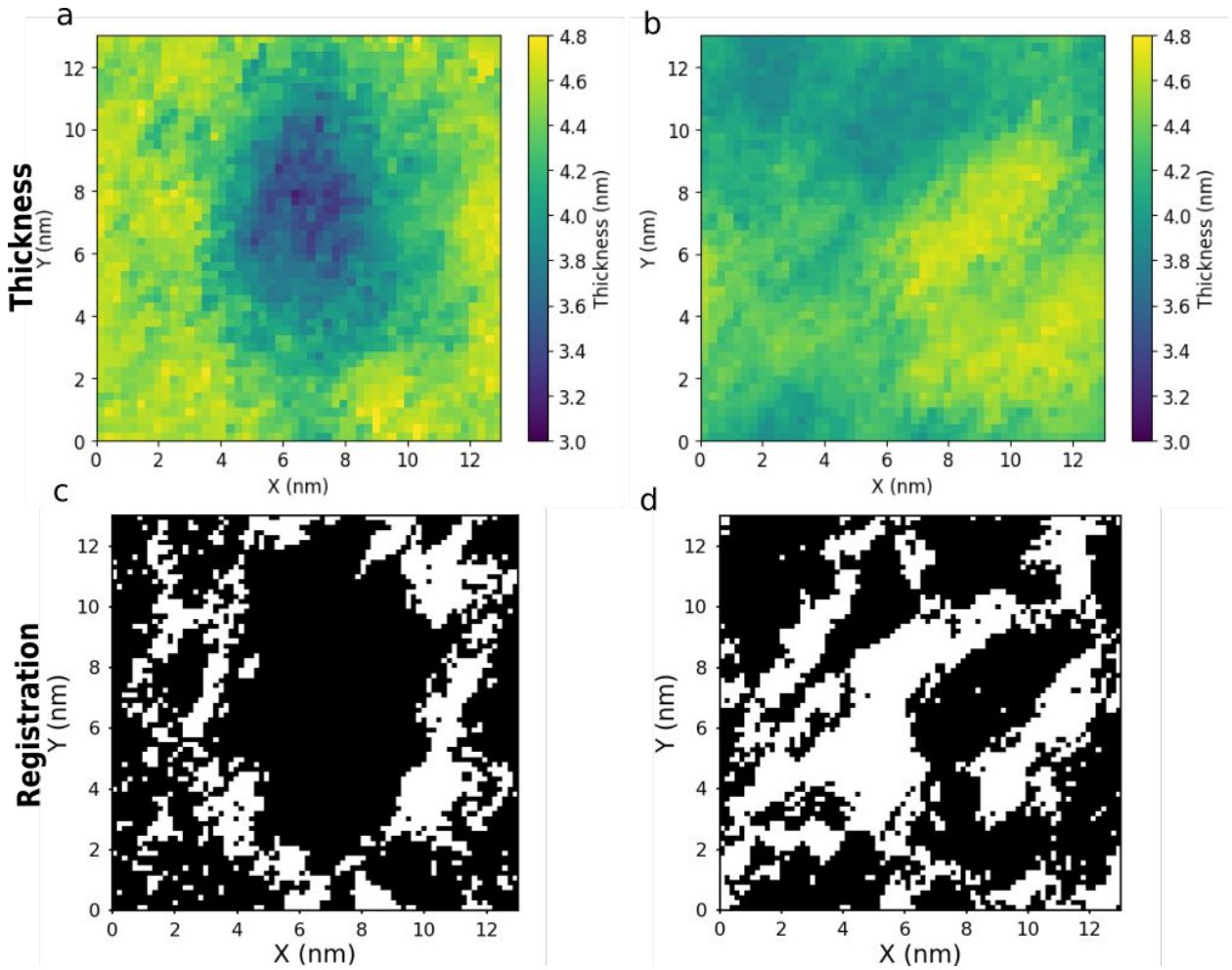

Figure S6. Membrane thickness and registration landscape of ternary membranes. Membrane thicknesses are computed as the distance between the PO4 beads of lipids. In the registration landscapes, the matched regions are marked by black color. Landscapes are sampled from 9.5 μs to 10 μs.

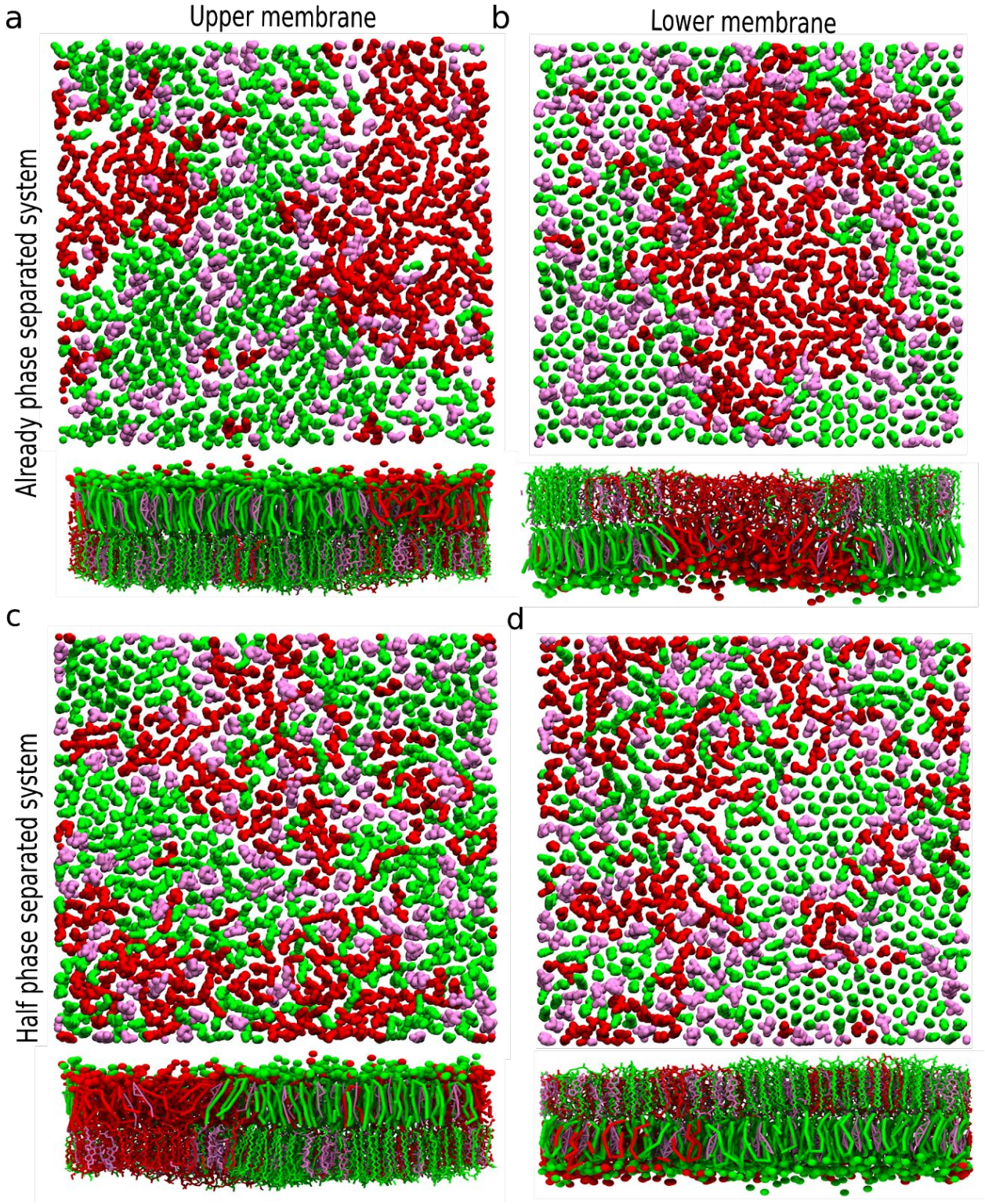

Figure S7. Top view of AA leaflets and the side view of bilayer in hybrid membrane systems. Only lipids tails are shown and the color scheme is the same as Figure 1.

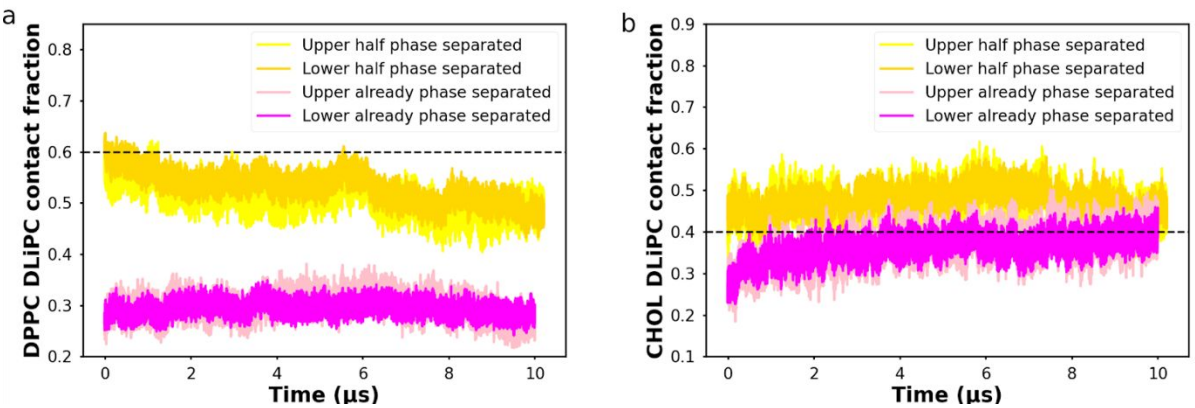

Figure S8. Lipid contact fraction for two membranes in hybrid systems. (a) DPPC-DLiPC contact fraction. The horizontal dashed line represents ideal mixing, above which DLiPC lipids prefer to contact DPPC lipids (more mixed), below which DLiPC lipids prefer contacts with themselves (more separated). (b) Contact fraction between cholesterol and DLiPC. The horizontal dashed line represents ideal mixing, above which cholesterol prefers to interact with DLiPC lipids, below which cholesterol prefers DPPC lipids. The 4 systems correspond to the snapshots in Figure S7.

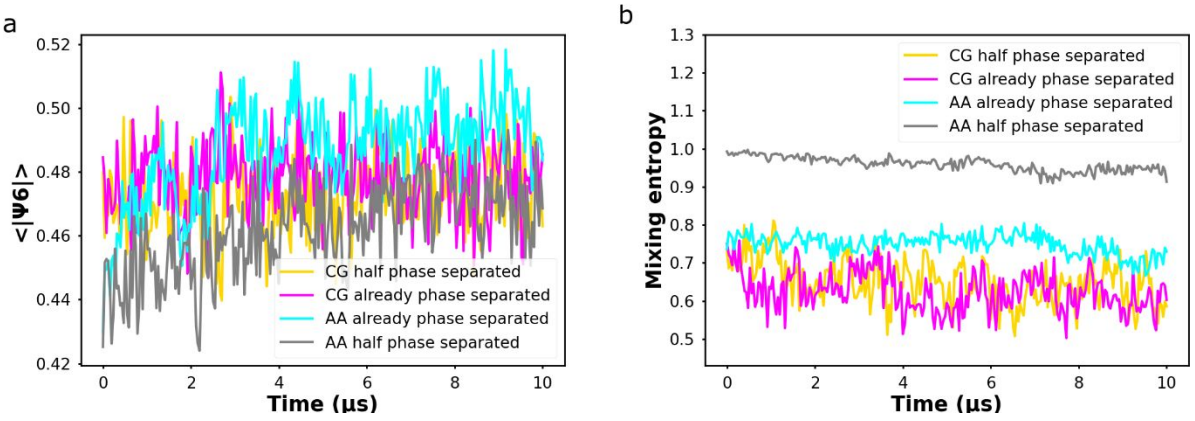

Figure S9. 2D bond-orientational order parameter ($|\Psi_6^k|$) and mixing entropy (S_{mix}) of upper membrane. (a) represents the averaged 2D bond-orientational order parameter and (b) represents the binary mixing entropy, where DPPC and DLiPC lipids are considered. The maximum value of S_{mix} is 1 (ideal mixing) and lower values are indicative of a more demixed phase. The higher $|\Psi_6^k|$ suggests a tighter packed or more hexatic-like lipid arrangement. For both systems, starting from the half and already phase separated membranes, the S_{mix} of CG leaflets fluctuate around 0.6 and $|\Psi_6^k|$ around 0.47, indicating these leaflets keep the demixed structure and the lipid arrangement barely change. For AA leaflet starting from already phase separated phase, the mixing entropy is higher than the opposite CG leaflet, suggesting a less phase separated state. While for the AA leaflet starting from the mixing phase, the mixing entropy decrease from 1, meaning the system starts to phase separate. These observations agree with the conclusions draw from

the DPPC-DLiPC contact fraction in Figure 3a. The $|\Psi_6^k|$ of both AA leaflets in two systems increase and reach a plateau after about 5 μs, indicating the AA lipids adopted a more packed arrangement. This finding agrees with the observation from Figure 5a and 5b that the local hexagonal arrangement in the DPPC-rich region is formed in both AA leaflets in two systems.

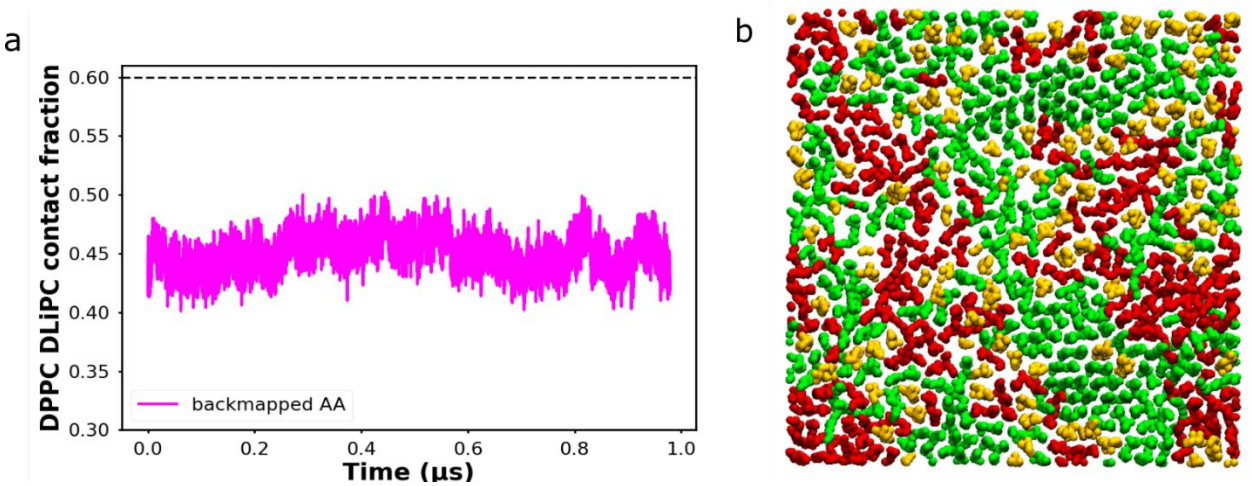

Figure S10. Phase separation level of the backmapped half phase separated AA system. (a) DPPC-DLiPC contact fraction. The horizontal dashed line represents ideal mixing, above which DLiPC lipids prefer to contact DPPC lipids (more mixed), below which DLiPC lipids prefer contacts with themselves (more separated). (b) represents the snapshot of the final state at $1\mu s$. Only lipids tails are shown and the color scheme is the same as Figure 1.

Table S1. Structural properties of different membranes at 295K

Resolution	Lipids	Lipid ratios	Area per lipid (nm^2)	Membrane thickness (nm)
AA	DLiPC	-	0.736±0.008	3.46±0.03
CG	DLiPC	-	0.735±0.010	3.58±0.05
VS hybrid	DLiPC	-	0.717±0.005	3.62±0.05
AA	DPPC/CHOL	61/37	0.430±0.008	4.56±0.02
CG	DPPC/CHOL	61/37	0.421±0.001	4.48±0.02
VS hybrid*	DPPC/CHOL	61/37	0.418±0.003	4.45±0.02
AA	DLiPC/CHOL	41/9	0.590±0.004	3.84±0.02
CG	DLiPC/CHOL	41/9	0.634±0.003	3.61±0.05
VS hybrid*	DLiPC/CHOL	41/9	0.595±0.002	3.87±0.02

* The C6 of the LJ potential between the cholesterols (R1-R5 beads) and the other leaflet is set to zero, while keeping the C12 unchanged.

** All the simulations last for more than 50 ns.

Table S2. Structural properties of fully AA membranes simulated using different force fields

Force field	Lipids	Lipid ratios	Temperature (K)	Area per lipid (nm^2)
In-house GROMOS*	DLiPC	-	295	0.737±0.004
CHARMM 36	DLiPC	-	295	0.691±0.004
In-house GROMOS*	DLiPC	-	303	0.751±0.004
CHARMM36**	DLiPC	-	303	0.707 ± 0.02
GROMOS 43A1-S3***	DLiPC	-	303	0.650±0.005
In-house GROMOS*	DLiPC/CHOL	41/9	295	0.590±0.004
CHARMM 36	DLiPC/CHOL	41/9	295	0.599±0.004
In-house GROMOS*	DLiPC/CHOL	1/1	303	0.454±0.005
GROMOS 43A1-S3**	DLiPC/CHOL	1/1	303	0.443±0.002

* The in-house GROMOS force field is described and tested in[2]. The area per lipid of DLiPC as a function of time is shown in Figure S4.

**The membrane properties are obtained from [3]

***The membrane properties are obtained from[4]

Reference

1. Alessandri, R.; Telles de Souza, P. C.; Thallmair, S.; Melo, M. N.; De Vries, A. H.; Marrink, S. J., Pitfalls of the Martini Model. *J. Chem. Theory Comput.* **2019**. *15.10*: 5448-5460.
2. Liu, Y.; De Vries, A. H.; Barnoud, J.; Pezeshkian, W.; Melcr, J.; Marrink, S. J., Dual Resolution Membrane Simulations Using Virtual Sites. *J. Phys. Chem. B* **2020,** *124* (19), 3944-3953.
3. Zhuang, X. Computational simulations on membranes and a transmembrane protein. 2017.
4. Emami, S.; Azadmard-Damirchi, S.; Peighambardoust, S. H.; Hesari, J.; Valizadeh, H.; Faller, R., Molecular dynamics simulations of ternary lipid bilayers containing plant sterol and glucosylceramide. *Chem. Phys. Lipids* **2017,** *203*, 24-32.